PHYSICAL REVIEW D **83,** 013006 (2011)

Pion transverse charge density from timelike form factor data

G. A. Miller,[1] M. Strikman,[2] and C. Weiss[3]

[1]*Department of Physics, University of Washington, Seattle, Washington 98195-1560, USA*
[2]*Department of Physics, Pennsylvania State University, University Park, Pennsylvania 16802, USA*
[3]*Theory Center, Thomas Jefferson National Accelerator Facility, Newport News, Virginia 23606, USA*

(Received 9 December 2010; published 25 January 2011)

The transverse charge density in the pion can be represented as a dispersion integral of the imaginary part of the pion form factor in the timelike region. This formulation incorporates information from e^+e^- annihilation experiments and allows one to reconstruct the transverse density much more accurately than from the spacelike pion form factor data alone. We calculate the transverse density using an empirical parametrization of the timelike pion form factor and estimate that it is determined to an accuracy of $\sim 10\%$ at a distance $b \sim 0.1$ fm, and significantly better at larger distances. The density is found to be close to that obtained from a zero-width ρ meson pole over a wide range and shows a pronounced rise at small distances. The resulting two-dimensional image of the fast-moving pion can be interpreted in terms of its partonic structure in QCD. We argue that the singular behavior of the charge density at the center requires a substantial presence of pointlike configurations in the pion's partonic wave function, which can be probed in other high-momentum transfer processes.

DOI: 10.1103/PhysRevD.83.013006 PACS numbers: 13.40.Gp, 11.55.Fv, 13.60.Hb, 13.66.Bc

I. INTRODUCTION

Learning to describe the structure and interaction of hadrons on the basis of QCD is one of the main objectives of nuclear physics. An essential step in this program is to understand the structure of the pion, a nearly massless excitation of the QCD vacuum with pseudoscalar quantum numbers. The pion plays a central role in nuclear physics as the carrier of the long-range force between nucleons and a harbinger of spontaneous symmetry breaking. The importance of the pion has been recognized by intense experimental and theoretical activity aimed at measuring its properties and understanding its structure. The pion electromagnetic form factor $F_\pi(t)$ was measured at spacelike momentum transfers through pion-electron scattering [1,2] and pion electroproduction on the nucleon [3–6]; new measurements in the region $|t| \sim$ few GeV^2 are planned with the Jefferson Lab 12 GeV Upgrade [7]. In the timelike region the modulus of the (complex) pion form factor, $|F_\pi(t)|$, was determined in a series of e^+e^- experiments [8–12]; see Ref. [13] for a compilation of the older data.

The concept of transverse densities [14], whose properties were explored in several recent works [15,16], provides a model-independent way to relate the form factors of hadrons to their fundamental quark/gluon structure in QCD. Defined as the 2-dimensional Fourier transforms of the elastic form factors, the transverse densities describe the distribution of charge and magnetization in the plane transverse to the direction of motion of a fast hadron; see Ref. [17] for a review. They are closely related to the parton picture of hadron structure in high-energy processes and correspond to a reduction of the generalized parton distributions (or GPDs) describing the distribution of quarks/antiquarks with respect to longitudinal momentum and transverse position [18,19]. It is therefore natural to attempt to interpret the pion form factor data in terms of the transverse charge density in the pion. In particular, the density at small transverse distances $b \ll 1$ fm places constraints on the probability of pointlike configurations (or PLCs) in the pion, i.e., $q\bar{q}$ configurations in the partonic wave function of a transverse size much smaller than the typical hadronic radius [20]. Such configurations play an important role in high-momentum transfer reactions involving pions, such as the pion transition form factor $\gamma^*\gamma \to \pi^0$ [21,22] or pion production in large-angle scattering processes [23]. They are essential for the physics of the color transparency phenomenon predicted by QCD [24,25], which is studied in high-energy pion dissociation on nuclear targets [26,27] and electromagnetic pion knockout [28,29] and is closely related to the existence of factorization theorems for hard meson production processes. The dynamical origin of PLCs—whether they are generated through perturbative QCD interactions with large-size configurations or by nonperturbative mechanisms—remains a subject of intense study.

The transverse charge density in the pion is defined as the 2-dimensional Fourier transform of the spacelike pion form factor,

$$\rho_\pi(b) = \int_0^\infty \frac{dQ}{2\pi} QJ_0(Qb)F_\pi(t = -Q^2), \qquad (1)$$

where F_π is regarded as a function of the invariant momentum transfer t. The function $\rho_\pi(b)$ gives the probability that charge is located at a transverse separation b from the transverse center of momentum, with $\int d^2b\rho_\pi(b) = 1$. The definition Eq. (1) may in principle be used to calculate the charge density directly from the spacelike form factor data. In the nucleon case, where the spacelike form factors

can be extracted directly from the measured eN elastic scattering cross section and are known up to rather large momentum transfers, this approach has been quite successful; see Ref. [30] for an assessment of the uncertainties. In the pion case the spacelike form factor at momentum transfers above $Q^2 > 0.25$ GeV^2 was extracted only indirectly in electroproduction experiments on the nucleon $N(e, e'\pi)N'$, with substantial model dependence, and is known only poorly at higher Q^2, rendering such a program difficult. However, for the pion one has another avenue for evaluating the transverse density, based on a dispersion representation for the pion form factor. Noting that the singularities of $F_\pi(t)$ as an analytic function of t are confined to a cut along the positive real axis starting at $t = 4m_\pi^2$, the form factor can be expressed as [31]

$$F_\pi(t) = \int_{4m_\pi^2}^{\infty} \frac{dt'}{t' - t - i0} \frac{\mathrm{Im} F_\pi(t')}{\pi}. \tag{2}$$

The asymptotic behavior expected from perturbative QCD, $F_\pi(t) \sim \alpha_s(t)/|t|$ for $t \to \infty$, allows the use of an unsubtracted dispersion relation [32]. Substitution of Eq. (2) in Eq. (1) leads to the result [33]

$$\rho_\pi(b) = \int_{4m_\pi^2}^{\infty} \frac{dt}{2\pi} K_0(\sqrt{t}b) \frac{\mathrm{Im} F_\pi(t + i0)}{\pi}. \tag{3}$$

This representation of the charge density as a dispersion integral over the imaginary part (or spectral function) of the timelike pion form factor has an interesting ''filtering'' property. The exponential dropoff of the modified Bessel function K_0 at large arguments causes the integrand of Eq. (3) to decrease exponentially at large t and ensures that only values $\sqrt{t} \sim 1/b$ in the spectral function are effectively sampled at a given distance b. In the nucleon case the timelike form factor is measurable only at $t > 4m_N^2$, and Eq. (3) is not useful for calculating the transverse density from data (it is, however, very useful for theoretical analysis; for example, the chiral large-distance component of the nucleon charge density at $b \sim m_\pi^{-1}$ can be obtained from the calculable strength of the two-pion cut in the nucleon form factor near threshold [33]). In the pion case the physical region for the timelike form factor starts at $t = 4m_\pi^2$, covering the entire range of the dispersion integral, and Eq. (3) becomes a practical method for calculating the charge density at all values of b. High-quality e^+e^- annihilation data exist for values of t up to $\sim$1 GeV^2, so that we hope to be able to determine $\rho_\pi(b)$ accurately for values of b at least down to values of $b \sim 1$ GeV$^{-1} = 0.2$ fm.

The imaginary part of the pion form factor $\mathrm{Im} F_\pi(t)$ entering in the dispersion representation Eq. (3) is not measured directly in annihilation experiments. The $e^+e^- \to \pi^+\pi^-$ cross section is proportional to $|F_\pi(t)|^2$, and model-dependent input is generally needed to determine the phase. In the region of the ρ meson resonance this problem was studied extensively long ago and is under good theoretical control. The phase of the first higher resonance ρ' is strongly constrained by the dispersion integrals (sum rules) for the pion charge and the measured charge radius. At larger values of t arguments based on perturbative QCD and local duality provide some guidance. Combined with the filtering property of the dispersion integral Eq. (3), these constraints strongly reduce the model dependence in the transverse density at $b \gtrsim 0.1$ fm. Our estimates below show that this way of constructing $\rho_\pi(b)$ gives substantially more accurate results than use of the spacelike pion form factor data alone.

In this article we calculate the transverse charge density in the pion in the dispersion representation Eq. (3) using an empirical parametrization of the timelike pion form factor based on e^+e^- annihilation and spacelike form factor data [34]. We find that the density is determined to an accuracy of $\sim$10% at transverse distances $b \sim 0.1$ fm, and substantially better at larger values. We thus obtain a precise 2-dimensional image of the fast-moving pion, which can be interpreted in terms of its partonic structure in QCD. In particular, the density exhibits a pronounced rise at small b, as was observed earlier—although with much lower precision—in an analysis based on the spacelike pion form factor [16]. Using experimental information on the quark density in the pion, we argue that such singular behavior of the charge density cannot be explained by large-size, $x \to 1$ configurations in the pion's partonic wave function and must therefore be attributed to PLCs. Our result thus places constraints on the probability of PLCs in the pion, which can be probed in other high-momentum-transfer processes involving pions.

The plan of this paper is as follows. In Sec. II we briefly describe the main features of the pion form factor in the timelike region and the elements of the parametrization of Ref. [34]. In Sec. III we calculate the transverse charge density and investigate its uncertainties at small distances. The implications for the pion's partonic structure and the presence of PLCs are discussed in Sec. IV. Section V discusses the possible role of chiral dynamics in the pion transverse density at large distances. A summary and suggestions for further studies are presented in Sec. VI.

II. TIMELIKE FORM FACTOR PARAMETRIZATION

In the energy region $\sqrt{t} \lesssim 1$ GeV the measured pion form factor $|F_\pi(t)|^2$ is dominated by the ρ meson resonance, with clearly visible effects of ρ-ω mixing (see Ref. [34] for a summary of the data). Theoretical support for ρ dominance at the amplitude level comes from the observation that the 2π channel accounts for most of the annihilation cross section, which allows one to relate the pion form factor to the $\pi\pi$ scattering amplitude via elastic unitarity. In this region the form factor is successfully described by the Gounaris-Sakurai (GS) amplitude [35], which is derived from an effective range expansion

of the $\pi\pi$ phase shift and has the correct analytic structure. The neglect of certain off-shell terms $\propto (t - m_\rho^2)$ in the GS amplitude leads to a Breit-Wigner (BW) type parametrization with energy-dependent width; this simplified form also describes the $|F_\pi(t)|^2$ data in the region $\sqrt{t} \lesssim 1$ GeV but does not respect the analytic properties of the form factor (it has a spurious branch cut singularity at $t = 0$). We shall employ the full GS parametrization in our studies here.

Above the ρ region, data for $|F_\pi(t)|^2$ exist up to energies $\sqrt{t} \lesssim 3$ GeV. Because of the many hadronic channels in the total cross section, the phase of the form factor at these energies is much more uncertain. In the region of the first higher resonance ρ' the phase is constrained by the sum rules for the pion charge and the charge radius, which require partial compensation of the spectral strength in the ρ meson region. At higher energies theoretical constraints come from the asymptotic behavior predicted by perturbative QCD, which demands strong cancellations between higher resonances in a resonance-based description, as indeed found in dual resonance models.

In the present study we use the timelike pion form factor parametrization of Ref. [34], which describes the high-energy region by a pattern of resonances consistent with the QCD asymptotic behavior. The parameters were determined by a detailed analysis of the timelike data up to $\sqrt{t} \lesssim 3$ GeV. The continuation of these parametrizations to $t < 0$ also describes the spacelike form factor in accordance with the data, including the recent JLab data up to $|t| = 2.45$ GeV^2 [6], which appeared after publication of Ref. [34].

A brief description of the elements of the parametrization of Ref. [34] is provided here; for details we refer to the original article and references therein. The first four ρ meson resonances are included as specific states with masses up to 2.0 GeV (ρ-ω mixing is taken into account for the lowest resonance). These resonances are described by the GS form, which incorporates the proper threshold behavior of the widths and has the correct analytic properties [36]. In addition, an infinite series of higher excitations is included via an ansatz [37] based on the dual resonance model. Its continuation to the spacelike region exhibits a smooth behavior with a power-law asymptotics as $|t|^{1-\beta}$, with $\beta = 2.1$–2.3. The imaginary part of the form factor obtained with the GS parametrization [34] is shown in Fig. 1(a) (solid line). One clearly sees the dominance of the ρ meson pole in the region $\sqrt{t} < 1$ GeV, and the alternating sign of successive resonance contributions at larger values of $\sqrt{t}$, as expected from theoretical considerations.

To estimate the uncertainty in the imaginary part, we have taken the quoted variances of the fit parameters of Ref. [34] and studied the statistical variation of the imaginary part, assuming uncorrelated errors. The resulting $\pm 1\sigma$ error band is shown in Fig. 1(a) (dotted lines). The

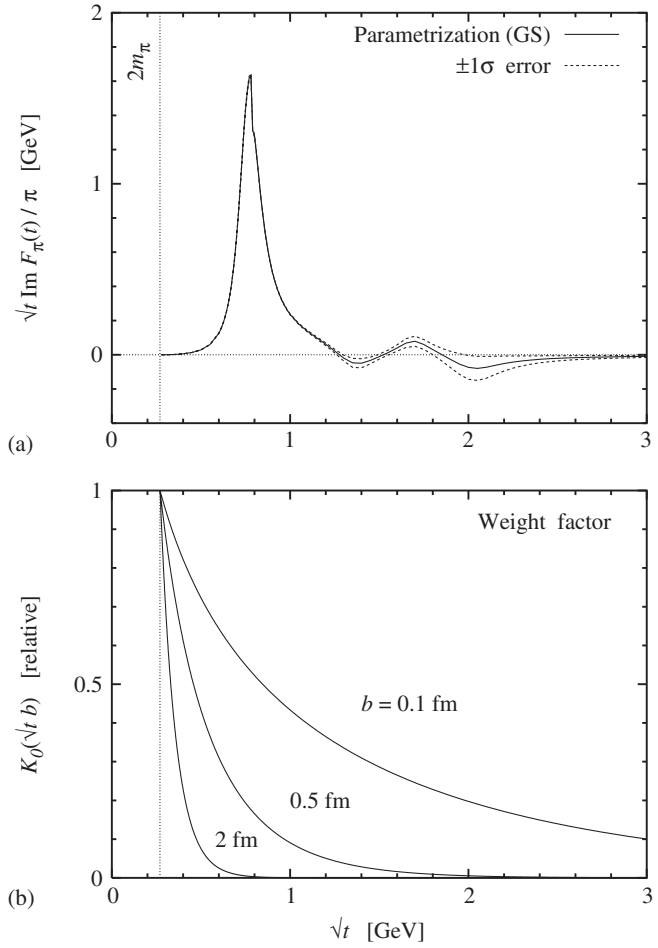

FIG. 1. (a) Solid line: the imaginary part of the pion form factor obtained from the fit of Ref. [34] (GS parametrization), as a function of $\sqrt{t}$. Shown here is the function $\sqrt{t}\,\mathrm{Im}F_\pi(t)/\pi$, which effectively enters in the dispersion integral over $\sqrt{t}$, Eq. (3). Dotted lines: $\pm 1\sigma$ error resulting from the uncorrelated uncertainties of the fit parameters. The threshold energy $\sqrt{t} = 2m_\pi$ is indicated by the vertical line. (b) The weight factor $K_0(\sqrt{t}b)$ in the dispersion representation of the transverse charge density Eq. (3), as a function of $\sqrt{t}$, for several values of b. Shown are the functions normalized to unity at the threshold $\sqrt{t} = 2m_\pi$.

variance in the ρ meson mass region is at the few percent level. At energies above 1 GeV it becomes substantially larger, reaching close to 100% at $\sqrt{t} = 2$ GeV. Note that in this energy region our uncorrelated estimate likely represents an upper bound on the uncertainty; for example, correlations between the statistical fluctuations of the coupling and width of the second resonance would considerably reduce the overall fluctuations of the imaginary part near $\sqrt{t} \sim 1.4$ GeV. For energies above 3 GeV we cannot reliably estimate the relative uncertainty of the imaginary part in this way, as the couplings of the resonances in this region are dictated by the dual resonance model, and the data in this region are very poor. However, the imaginary part in this region is expected to be very small and

contributes negligibly to the charge density at $b > 0.1$ fm (see below), so that its relative uncertainty is not important for our purposes. We emphasize that we use the parametrization of Ref. [34] only as an effective representation of $\mathrm{Im}F_\pi(t)$ in the energy range $\sqrt{t} < 3$ GeV, and that our conclusions do not depend on the particular $\sqrt{t} \to \infty$ asymptotic behavior imposed by the dual resonance model.

III. TRANSVERSE DENSITY AND ITS UNCERTAINTY

We now use the timelike form factor parametrization to evaluate the transverse charge density in the pion and estimate its uncertainty. It is instructive to study first the distribution of strength in the dispersion integral Eq. (3). The imaginary part $\mathrm{Im}F_\pi(t)$ is weighted with the modified Bessel function $K_0(\sqrt{t}b)$, which exponentially suppresses energies $\sqrt{t} \gg 1/b$. Figure 1(b) shows this weight factor as a function of $\sqrt{t}$ for several values of b, normalized to the same value at threshold $\sqrt{t} = 2m_\pi$, i.e., the ratio

$$K_0(\sqrt{t}b)/K_0(2m_\pi b). \tag{4}$$

One sees that the effective distribution of strength in $\sqrt{t}$ strongly changes with the distance b. At $b = 0.1$ fm a noticeable contribution to the dispersion integral comes from the region $\sqrt{t} > 1$ GeV, where the parametrization of $\mathrm{Im}F_\pi(t)$ shows considerable uncertainty [see Fig. 1(a)]. At $b = 0.5$ fm these contributions are largely suppressed, resulting in almost perfect "vector meson dominance" in the dispersion integral. Finally, going to distances as large as $b \sim 2$ fm, one begins to suppress also the ρ mass region and emphasizes the near-threshold region of the form factor, $\sqrt{t} - 2m_\pi \sim$ few m_π.

In order to quantify the accuracy of the calculated transverse density we need to study the numerical convergence of the dispersion integral at large values of $\sqrt{t}$. Figure 2 shows the percentage deviation of $\rho_\pi(b)$ from the full result as a function of a cutoff applied to the upper limit of the $\sqrt{t}$ integral in Eq. (3) (here the integral is evaluated with the central value of the GS parametrization as shown in Fig. 1). One sees that at $b = 0.1$ fm the region $\sqrt{t} > 3$ GeV accounts for only about $\sim$1% of the total integral, meaning that even a drastic change of $\mathrm{Im}F_\pi(t)$ in this region by a factor 2–3 would change the density only by $\sim$2–3% [38]. The error in the density is thus dominated by the mass region $1 < \sqrt{t} < 3$ GeV, where we have estimated the uncertainty of $\mathrm{Im}F_\pi(t)$ in Sec. II. With a $\sim$100% uncertainty at $\sqrt{t} = 2$ GeV, where the integral has converged to within $\sim$4% of its value, we expect an uncertainty of the density of (at least) $\sim$4%. Surprisingly, even for much smaller distances the region $\sqrt{t} > 3$ GeV seems to contribute relatively little to the dispersion integral; see the curve in Fig. 2 for $b \sim 0.02$ fm. While the integral requires larger values of $\sqrt{t}$ to converge, the contribution from $\sqrt{t} > 3$ GeV is still only $\sim$2%, and the overall uncertainty can be estimated from

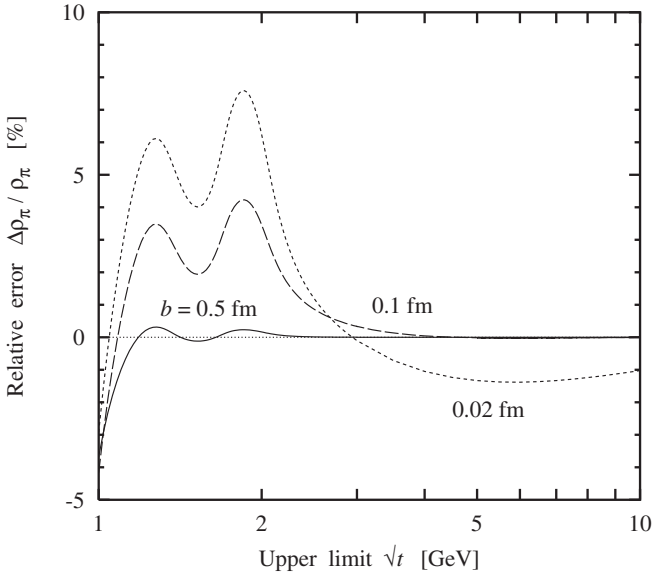

FIG. 2. Percentage deviation from the full result for the dispersion integral Eq. (3), as a function of the upper limit of $\sqrt{t}$, for $b = 0.5$ fm (solid line), 0.1 fm (dashed line), and 0.02 fm (dotted line). The integrand is evaluated using the GS parametrization of Ref. [34].

that of the region $1 < \sqrt{t} < 3$ GeV. At larger distances $b \sim 0.5$ fm, the integral has fully converged already at $\sqrt{t} \sim 1$ GeV, and the overall uncertainty is dominated by the low-energy region $\sqrt{t} < 1$ GeV. In this region the parameter errors in the fit are so small that the model dependence of the parametrizations (details of ρ-ω mixing, ρ line shape) can no longer be neglected in establishing the overall error.

Given the dominance of energies $\sqrt{t} < 3$ GeV in the dispersion integral, we can evaluate the density with the parametrization of Ref. [34] and estimate its uncertainty from the parameter error band shown in Fig. 1 The result is displayed in Fig. 3. The quoted 1σ error in $\mathrm{Im}F_\pi(t)$ translates into an uncertainty of $\rho_\pi(b)$ of $\pm(1.5, 7, 13)\%$ at $b = (0.5, 0.1, 0.02)$ fm. The density is thus determined much more accurately, and down to much smaller distances, than from the spacelike pion form factor data alone [16].

A welcome feature of the dispersion representation of the charge density, Eq. (3), is that the kernel $K_0(\sqrt{t}b)$ is a positive function. As a result, an upper or lower bound on the spectral function $\mathrm{Im}F_\pi(t)$ directly provides a corresponding bound on $\rho_\pi(b)$, greatly simplifying the error analysis. (A method to estimate the uncertainty of the charge density as the Fourier transform of the spacelike form factor was described in Ref. [30].)

An additional source of uncertainty in the charge density at small distances are recent data on the timelike pion form factor at large values of t that were not included in the fit of Ref. [34]. The CLEO measurement [12] at $\sqrt{t} = 3.67$ GeV

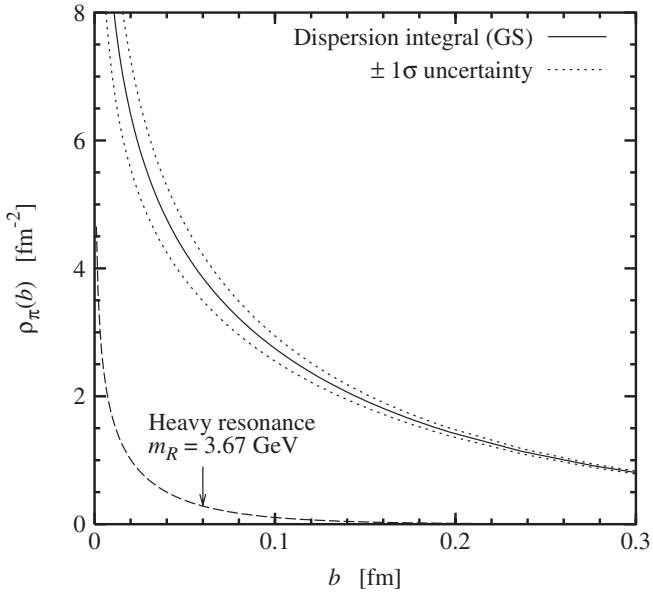

FIG. 3. Transverse charge density in the pion, $\rho_\pi(b)$. Solid line: dispersion integral Eq. (3) evaluated with the GS form factor parametrization [34] [see Fig. 1(a)]. Dotted lines: 1σ error resulting from the quoted uncertainty of the parametrization [see Fig. 1(a)]. Dashed line: density resulting from a heavy resonance with mass $m_R = 3.67$ GeV and width $\Gamma_R = 0.2\ m_R$, providing a rough assessment of the impact of the CLEO timelike form factor data [12] (for details, see text).

reports a value of $|F_\pi| = 0.075 \pm 0.008(\text{stat}) \pm 0.005(\text{syst})$, much larger than the value 0.034 provided by the GS parametrization of Ref. [34]. We see no simple way to modify the parametrization to account for this datum. Indeed, Ref. [34] argues that increasing the absolute value of the form factor by a factor of ~ 2 at large $\sqrt{t}$ is not possible. In particular, the article states that it is implausible for the form factor obtained on the basis of a dual resonance parametrization to reach values $|F_\pi(t)|^2 \geq 0.01$ at $\sqrt{t} = 2.5$–3 GeV (as would correspond to the new datum, assuming powerlike t-dependence) without conflicting with the spacelike data and especially with QCD predictions [39].

One possibility is that the error of the CLEO result is larger than estimated in Ref. [12]. Another possibility is that there is a new mechanism providing a strong coupling to two pions at high energies. Here we only wish to make a rough assessment of the potential impact of this new datum on the transverse density. To this end, let us assume the existence of an "additional" $\pi\pi$ resonance at $\sqrt{t} = m_R \equiv 3.67$ GeV, described by the GS form, whose coupling c_R to the virtual photon is related to the measured pion form factor as

$$|F_\pi(m_R)| = c_R m_R/\Gamma_R. \tag{5}$$

Taking the width Γ_R to be $\sim 20\%$ of the mass, as it is for the ρ meson, we obtain a coupling $c_R = 0.015$ from the CLEO measurement. Such an addition gives a negligible contribution to $|F_\pi(t)|$ at the values of $\sqrt{t}$ for which most of the data entering in the parametrization [34] were taken; for example, it provides a $\sim 1\%$ contribution to $|F_\pi(t)|$ at $\sqrt{t} = 1$ GeV. The "extra" contribution to the charge density from such a resonance would be $+(0.04,\ 4,\ 16)\%$ at $b = (0.5,\ 0.1,\ 0.02)$ fm (see Fig. 3). If we added this uncertainty to the one estimated previously from the error of the parametrization for $\sqrt{t} < 1$ GeV, we would conclude that the density is determined to $(\pm 1.5,\ +11-7,\ +39-16)\%$ at the quoted values of b. This is surely a conservative estimate, as at least part of the uncertainty in the unmeasured high-t region is already included in the parametrization error. A larger value of the width of the hypothetical resonance would lead to a proportionately larger contribution to $\rho_\pi(b)$, but would have to be reconciled with the precise data for $|F_\pi|$ in the mass region $\sqrt{t} \lesssim 1$ GeV. We conclude that the new CLEO data have only a modest impact on the transverse density at distances ~ 0.1 fm, but may cause substantial modifications at smaller distances.

Figure 4 shows the transverse density obtained from the dispersion integral on a logarithmic scale, which allows one to see the exponential falloff at larger distances. For comparison we also show the density obtained from a single resonance of zero width at the ρ meson mass m_ρ, with a coupling chosen to ensure unit charge (i.e., the vector meson dominance model)

$$\rho_\pi(b)_{\text{zero-width}} = (m_\rho^2/2\pi) K_0(m_\rho b). \tag{6}$$

One sees that the dispersion result is very close to the zero-width ρ form for all distances $0.1 < b < 1$ fm and can be

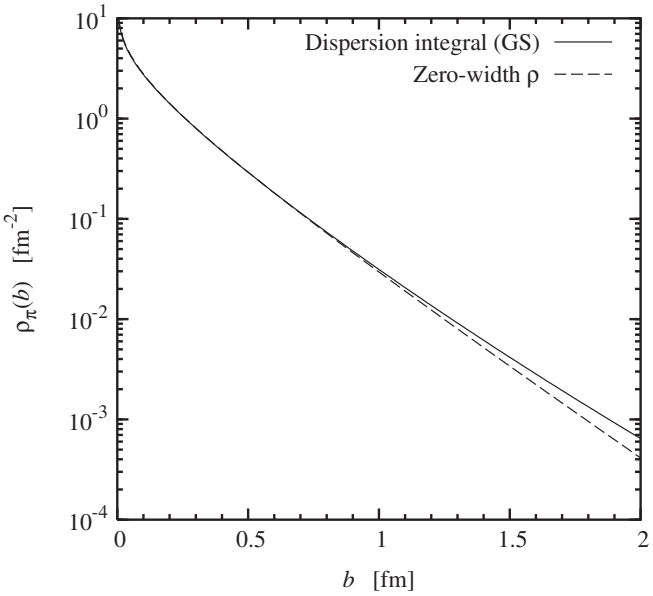

FIG. 4. Transverse charge density $\rho_\pi(b)$ in the pion. Solid line: dispersion integral Eq. (3) evaluated with the GS form factor parametrization of Ref. [34]. Dashed line: density from zero-width ρ meson pole, Eq. (6).

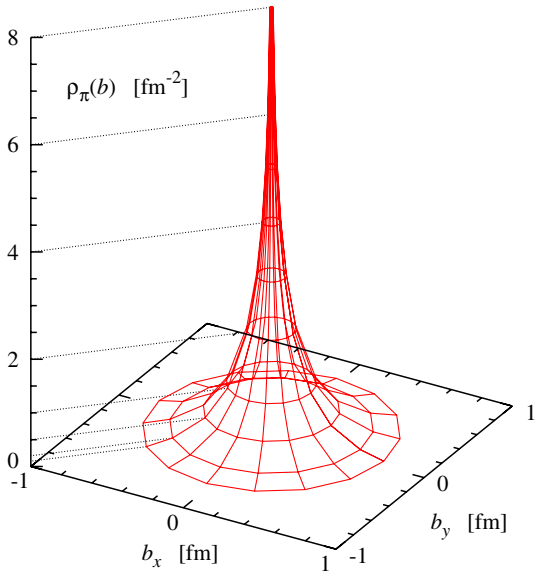

FIG. 5 (color online). Three-dimensional rendering of the transverse charge density in the pion, as obtained from the dispersion integral Eq. (3) evaluated with the GS form factor parametrization of Ref. [34]; cf. Figs. 3 and 4.

represented by the latter within the estimated errors (at larger values of b the spectral strength near threshold becomes important; see Sec. V). What is more, the dispersion result follows the zero-width ρ curve down to much smaller distances, being only a few percent smaller down to $b = 0.01$ fm. This shows that there are very strong cancellations between the effective poles parametrizing the high-mass continuum. As we just demonstrated, there is considerable uncertainty in the dispersion result for the density at such small distances. However, there is the intriguing possibility that the density might effectively be described by vector meson dominance down to distances significantly smaller than the inverse ρ meson mass, $m_\rho^{-1} = 0.25$ fm.

In Fig. 5 we show a 3-dimensional rendering of the transverse charge density, which conveys also the information on the supporting area and thus gives an impression of the true physical shape of the fast-moving pion as seen by an electromagnetic probe. Our dispersion approach provides a data-based image of the pion's transverse structure at small distances with unprecedented precision. One clearly sees the strong rise of the transverse density toward the center. This remarkable observation calls for a microscopic explanation in terms of the pion's partonic structure.

IV. IMPLICATIONS FOR PION PARTONIC STRUCTURE

The results of our empirical study of the transverse charge density have interesting implications for the partonic structure of the pion in QCD. The transverse charge density puts constraints on the possible distribution of transverse sizes of configurations in the pion's partonic wave function. A useful quantity to consider is the integral of the transverse charge density up to a given distance,

$$P(b) \equiv \int d^2b' \Theta(b - b') \rho_\pi(b'), \tag{7}$$

which determines the cumulative probability for configurations contributing to the transverse density at the distance b. The probability obtained from our dispersion result for the charge density (cf. Figs. 3 and 4) is shown in Fig. 6, together with that obtained from a zero-width ρ meson pole [cf. Eq. (6)],

$$P(b)_{\text{zero-width}} = m_\rho b K_1(m_\rho b). \tag{8}$$

The probability reaches $1/2$ at $b = 0.33$ fm, a value somewhat smaller than the root of the mean squared (RMS) transverse radius, $\langle b^2 \rangle_\pi^{1/2} = 0.53$ fm. This is to be expected, as large-size configurations are counted with a higher weight in the average of b^2 than the median. The RMS transverse radius calculated from our dispersion integral for the charge density agrees very well with the value extracted from the slope of the low-t pion form factor measured in πe scattering experiments, $\langle r^2 \rangle_\pi = (3/2) \times \langle b^2 \rangle_\pi = 0.439 \pm 0.008$ fm^2 [1,2], as was already noted in the discussion of the fit to the timelike form factor data in Ref. [34].

To understand how the transverse charge density is related to the partonic structure it is necessary to recall

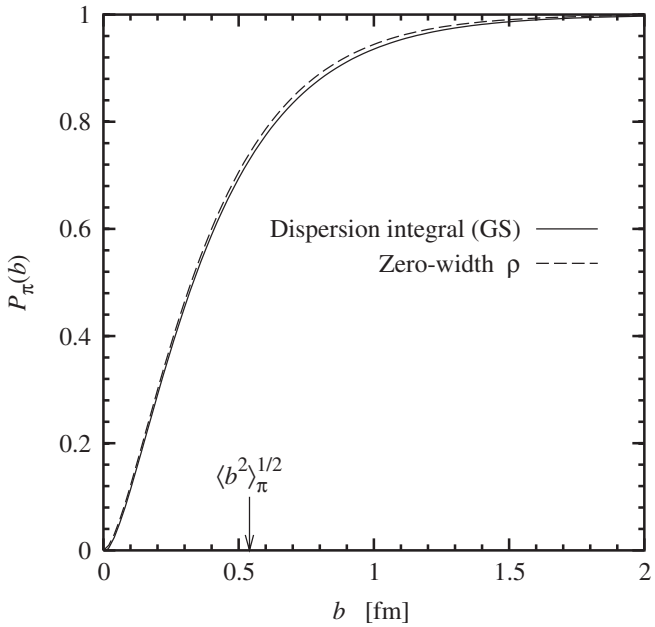

FIG. 6. Probability accumulation Eq. (7) in the transverse density (cf. Figs. 3 and 4). Solid line: dispersion integral (GS parametrization). Dashed line: zero-width ρ meson pole. The arrow indicates the experimental RMS transverse charge radius.

the relationship between the coordinate b and the physical transverse size of configurations in the fast-moving pion. The coordinate b measures the distance between a constituent—say, a quark q—and the transverse center of momentum of the pion. If the quark carries longitudinal momentum fraction x, and the remnant system R carries $1-x$, the transverse center of momentum of the pion is at $x\boldsymbol{r}_q + (1-x)\boldsymbol{r}_R$, where $\boldsymbol{r}_{q,R}$ denotes the transverse position of the quark and the center of momentum of the remnant system. The transverse separation of the quark from the remnant system is thus given by

$$r \equiv |\boldsymbol{r}_q - \boldsymbol{r}_R| = b/(1-x). \tag{9}$$

Figure 7 illustrates this relation for a $q\bar{q}$ configuration, in which the remnant system consists of a single antiquark. In the transverse charge density one considers the charge-weighted density of constituents at a given b, which is obtained as the average over configurations with different x and physical size r in the partonic wave function. Equation (9) now implies that the charge density at values of b much smaller than the typical hadronic size, $R_{\rm had} \sim 1$ fm, can arise from two different classes of configurations:

(I) Small physical size $r \ll R_{\rm had}$ and non-exceptional values of x, i.e., not close to 1 (PLCs). One expects the elementary $q\bar{q}$ configuration to account for a significant fraction of these configurations, as the emission of gluons and creation of additional $q\bar{q}$ pairs are suppressed in small-size color-singlet configurations. The existence of such PLCs is required by the nonzero value of the pion weak decay matrix element, parametrized by the constant f_π, where the axial current operator annihilates a $q\bar{q}$ pair in a point in space [21].

(II) Large physical size $r \sim R_{\rm had}$ and extreme momentum fractions $x \sim 1 - b/R_{\rm had}$ (end point configurations). These are generally not just $q\bar{q}$ configurations, as soft gluon radiation is not suppressed in large-size configurations. The probability of such configurations determines the behavior of the parton densities in the pion at large values of x.

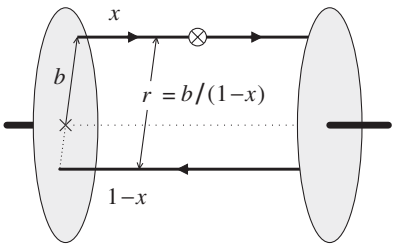

FIG. 7. Transverse distances in a $q\bar{q}$ configuration of the pion's partonic wave function: b is the distance between the quark and the transverse center of momentum, r the distance between the q and $\bar{q}$.

As with all analysis of partonic structure, the distinction between the two classes of configurations depends on the resolution scale Q^2. Standard leading-$\log Q^2$ evolution degrades the parton momentum fractions and reduces the probability of end point configurations. The total charge density resulting from the sum of all configurations is of course scale-independent, being the matrix element of a conserved current.

We can estimate the possible contribution of large-size $x \to 1$ configurations to the transverse density at small b in a simple phenomenological model, using information on the quark distribution in the pion at large x extracted from fits to πN Drell-Yan data [40]. Our basic assumption here is that the physical transverse size of large-x configurations in the pion tends toward a finite value of the order of the typical hadronic size. Generalizing the expression obtained from the overlap of light-cone wave functions of individual configurations, we model the x-and b-dependent charge density (i.e., the charge-weighted quark GPD) arising from large-x configurations as

$$\rho_\pi(x,b)_{\text{large-size}} = q_\pi(x)\frac{f(r=b/(1-x))}{(1-x)^2}, \tag{10}$$

where $q_\pi(x)$ is the valence quark distribution in the pion [41] and $f(r)$ describes the distribution over physical transverse sizes r, with a range of the order of the typical hadronic size, normalized such that $\int d^2 r f(r) = 1$; Eq. (10) thus satisfies $\int d^2 b \rho_\pi(x,b) = q_\pi(x)$. The transverse charge density $\rho_\pi(b)$ arising from large-size configurations is then given by the integral of the density Eq. (10) over x. In calculating this integral we impose the *physical* requirement that the transverse size r of the configuration be larger than some critical r_0. This limits the range of x in the integral to values $x > 1 - b/r_0$, where it is assumed that $b < r_0$. We thus consider the "conditional" large-size contribution to the density defined as

$$\rho_\pi(b|r>r_0) = \int_{1-b/r_0}^{1} dx \rho_\pi(x,b)_{\text{large-size}}. \tag{11}$$

To evaluate this contribution to the charge density at small b, we use the parametrization of the pion quark density of Ref. [42]. The size distribution $f(r)$ we take to be of Gaussian form, $f(r) = \exp(-r^2/R^2)/(\pi R^2)$, where the parameter $R^2 = \langle r^2 \rangle_\pi$ defines the average squared radius and is of the order of the typical hadronic size ~ 1 fm^2. For a loosely bound $q\bar{q}$ state with $\langle x \rangle_\pi = 1/2$ one would have $\langle r^2 \rangle_\pi = \langle b^2/(1-x)^2 \rangle_\pi \approx 4\langle b^2 \rangle_\pi$; a natural choice is therefore $R^2 = 4\langle b^2 \rangle_{\pi,\text{exp}} = 1.16$ fm^2. Figure 8 shows the contribution to the charge density from configurations with $r > r_0 = 0.2$ fm estimated with this model, for two values of Q^2. One sees that it accounts only for at most $\sim 20\%$ of the total transverse density at $b = 0.1$ fm, and even less at smaller distances. We thus conclude that large-size configurations with $x \to 1$ play only a minor role in the pion

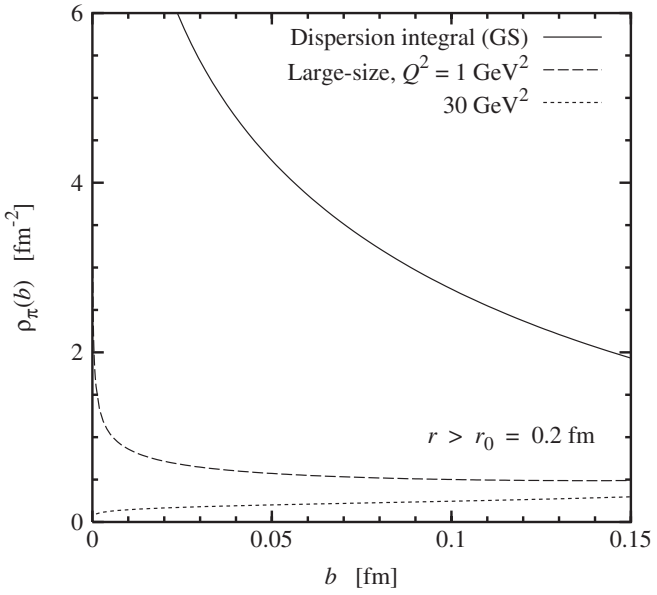

FIG. 8. Dashed/dotted line: contribution of large-size configurations with $r > r_0$ to the transverse charge density in the pion, as estimated in the model defined by Eqs. (10) and (11), for $r_0 = 0.2$ and two values of Q^2. Solid line: density obtained from the dispersion integral, cf. Fig. 3.

transverse charge density at small b, and that most of it can be attributed to PLCs.

The small-b behavior of the large-size contribution to the charge density in our model can formally be related to the power behavior of the quark distribution in the pion for $x \to 1$. In the limit of small b the integral in Eq. (11) extends over a narrow range of x close to 1. If the quark distribution vanishes as $q_\pi(x) \sim (1-x)^\beta$, one easily shows that the density Eq. (11) scales as $\rho_\pi(b|r > r_0) \sim b^{\beta-1}$ for $b \to 0$. The change in the small-b behavior with Q^2 seen in Fig. 8 reflects the effect of QCD evolution on the exponent β. Note, however, that even in the low-Q^2 region where $\beta < 1$ the large-size contribution in our model is substantially smaller than the total density obtained from the dispersion integral.

In sum, our estimate shows that large-size $x \to 1$ configurations cannot account for the strong rise of the transverse density at small b, and that it is therefore reasonable to interpret the empirical density in terms of PLCs in the pion's partonic wave function. In $q\bar{q}$ configurations of small size, it is expected that the wave function peaks at $x = 1/2$, which implies that the physical transverse size of the most likely configurations is $r \approx 2b$. With the plausible assumption that the small-size configurations in the pion are mostly $q\bar{q}$, we would conclude from Fig. 6 that there is a probability of 12% (29%) for configurations with $b < 0.1$ fm (0.2 fm), and thus with $q\bar{q}$ separation $r \lesssim 0.2$ fm (0.4 fm). In reality, some of these small-size configurations are $q\bar{q}$ + gluons or $qq\bar{q}\,\bar{q}$, requiring a detailed model-dependent analysis. Even so, our result for the charge density places strong constraints on the pion's partonic structure at small distances. The study of dynamical models of PLCs in the pion and their comparison with the empirical charge density will be the subject of future work.

V. LONG-RANGE PION STRUCTURE AND CHIRAL DYNAMICS

To complete our study of the empirical transverse charge density in the pion we briefly want to comment on the possible role of chiral dynamics at large transverse distances. At $b \gtrsim m_\pi^{-1} = 1.5$ fm the weighting factor $K_0(\sqrt{t}b)$ in the dispersion integral Eq. (3) emphasizes the near-threshold region $\sqrt{t} - 2m_\pi \sim$ few m_π [see Fig. 1(b)], where the imaginary part of the form factor is governed by chiral dynamics and calculable from first principles. In leading order of the chiral expansion, the imaginary part near threshold results from the pion loop graph with the $\pi\pi$ 4-point coupling and is given by [43–45]

$$\pi^{-1}\,\mathrm{Im}F_\pi(t + i0) = \frac{(t - 4m_\pi^2)^{3/2}}{6(4\pi f_\pi)^2\sqrt{t}}. \tag{12}$$

Substitution of this result in Eq. (3) allows one to derive the leading $\exp(-2m_\pi b)$ asymptotic behavior of the pion charge density at large distances; see Ref. [33] for details. Numerical analysis shows that the contribution from Eq. (12) to the charge density is negligible compared to the nonchiral density resulting from $\sqrt{t} \sim m_\rho$ for all but the largest distances, reaching only ~30% of the dispersion result at $b = 2$ fm. In the nucleon isovector charge density the chiral component was found to become comparable to the nonchiral density at distances $b \sim 1.7$ fm [33]; the reason for its diminished role in the pion charge density is that the triangle graph involving the πN Yukawa coupling (see Fig. 1 of [33]), which gave the main contribution in the nucleon case, is absent for the pion. Account of higher-order chiral corrections does not substantially change the magnitude of the chiral component [45]. We conclude that the transverse charge density in the pion is dominated by the ρ meson mass region for all distances of practical relevance, $b < 2$ fm.

VI. SUMMARY AND DISCUSSION

This paper shows how the pion form factor in the timelike region can be used to determine the transverse charge density. The timelike data greatly augment the meager information available from spacelike pion form factor measurements; in particular, in the region of high momentum transfers $|t| > 1$ GeV^2 conjugate to short transverse distances. Given the energy reach of the timelike form factor data, and the theoretical uncertainties involved in separating the real and imaginary parts, we estimate that $\rho_\pi(b)$ is determined to an accuracy of ~10% at $b = 0.1$ fm, and substantially better at larger distances.

The transverse density obtained from the full dispersion integral turns out to be surprisingly close to that obtained from a single zero-width ρ meson pole over a wide range. The empirical transverse density shows a strong rise at small distances, which points to a substantial presence of PLCs in the pion's partonic wave function and puts strong constraints on the pion GPD.

In the work reported here we limited ourselves to a phenomenological analysis of the transverse density based on an existing parametrization of the timelike pion form factor data. Our results suggest several directions for further studies, both theoretical and empirical.

The striking similarity of the empirical transverse density to the simple vector meson dominance model over a wide region of b should have a dynamical explanation. Possible approaches to addressing this question are local quark-hadron duality or the dual resonance picture of QCD in the large-N_c limit.

The strong rise of the pion's transverse charge density at small distances calls for an explanation in terms of dynamical models of the pion's partonic structure. The key question is whether the required PLCs in the pion could be explained as the result of perturbative QCD interactions with large-size configurations, or whether nonperturbative interactions play an essential role. Of particular interest for addressing this question are models which implement the nonperturbative short-distance scale associated with the spontaneous breaking of chiral symmetry in QCD such as the instanton vacuum model, which is known to give a reasonable description of the spacelike pion form factor at intermediate momentum transfers $Q^2 \sim$ few GeV^2 [46,47].

The dispersion result for the transverse charge density at distances $b \sim 0.1$ fm depends sensitively on the phase of the pion form factor in the region of the lowest excited ρ states, $\sqrt{t} = 1$–3 GeV. While the alternating sign of the coupling of successive resonances is suggested by theoretical considerations, it would be worthwhile to attempt independent experimental tests of this key assumption. This could be done through coherent photo- or electroproduction of two pions on nuclear targets, which can be analyzed in the spirit of the generalized vector meson dominance model; see Ref. [48] and references therein. Such measurements become feasible with the 12 GeV Upgrade of Jefferson Lab.

The recent CLEO data [12], which are difficult to explain in the dual resonance framework commonly used to parametrize the high-energy region of the pion form factor, may have a significant effect on the charge density at distances $b < 0.1$ fm. Confirmation of this experimental result and more data in the energy region $\sqrt{t} = 3$–4 GeV would certainly be welcome. It would be interesting to explore ways to include these data in a dispersion analysis with more general parametrizations of the imaginary part.

The new application of the timelike pion form factor described here once more underscores the importance of analyticity in relating observables measured in different kinematic regions. It would be helpful if phenomenological parametrizations of the form factors such as [34] employed a framework which strictly respects analyticity, e.g., by using analytic functions like the GS form, or by parametrizing only the spectral strength on the physical cut and generating the real part by a dispersion integral.

ACKNOWLEDGMENTS

G. A. M. acknowledges the hospitality of Jefferson Lab during the work on this study. This work is supported by the U.S. DOE under Grants No. DE-FGO2-97ER41014 and DE-FGO2-93ER40771. This work was supported by DOE Contract No. DE-AC05-06OR23177, under which Jefferson Science Associates, LLC, operates Jefferson Laboratory. The U.S. government retains a non-exclusive, paid-up, irrevocable, worldwide license to publish or reproduce this manuscript for U.S. Government purposes.

[1] E. B. Dally *et al.*, Phys. Rev. D **24**, 1718 (1981); E. B. Dally *et al.*Phys. Rev. Lett. **48**, 375 (1982).
[2] S. R. Amendolia *et al.*, Phys. Lett. B **146**, 116 (1984); S. R. Amendolia *et al.*(NA7 Collaboration), Nucl. Phys. **B277**, 168 (1986).
[3] C. J. Bebek *et al.*, Phys. Rev. D **13**, 25 (1976); C. J. Bebek *et al.*Phys. Rev. D**17**, 1693 (1978).
[4] H. Ackermann *et al.*, Nucl. Phys. **B137**, 294 (1978); P. Brauel *et al.*, Z. Phys. C **3**, 101 (1979).
[5] J. Volmer *et al.* (Jefferson Lab Fpi Collaboration), Phys. Rev. Lett. **86**, 1713 (2001); V. Tadevosyan *et al.* (Jefferson Lab Fpi Collaboration), Phys. Rev. C **75**, 055205 (2007).
[6] T. Horn *et al.* (Jefferson Lab Fpi-2 Collaboration), Phys. Rev. Lett. **97**, 192001 (2006); H. P. Blok *et al.* (Jefferson Lab Fpi-2 Collaboration), Phys. Rev. C **78**, 045202 (2008); G. M. Huber *et al.* (Jefferson Lab Fpi-2 Collaboration), Phys. Rev. C **78**, 045203 (2008).
[7] G. Huber, D. Gaskell (spokespersons), Jefferson Lab Experiment E12-06-101, ''Measurement of the Charged Pion Form Factor to High Q^2.''
[8] D. Bollini *et al.*, Lett. Nuovo Cimento Soc. Ital. Fis. **14**, 418 (1975).
[9] L. M. Barkov *et al.*, Nucl. Phys. **B256**, 365 (1985).
[10] D. Bisello *et al.* (DM2 Collaboration), Phys. Lett. B **220**, 321 (1989).
[11] R. R. Akhmetshin *et al.* (CMD-2 Collaboration), Phys. Lett. B **527**, 161 (2002); **578**, 285 (2004).

[12] T. K. Pedlar *et al.* (CLEO Collaboration), Phys. Rev. Lett. **95**, 261803 (2005).
[13] M. R. Whalley, J. Phys. G **29**, A1 (2003).
[14] D. E. Soper, Phys. Rev. D **15**, 1141 (1977).
[15] G. A. Miller, Phys. Rev. Lett. **99**, 112001 (2007).
[16] G. A. Miller, Phys. Rev. C **79**, 055204 (2009).
[17] G. A. Miller, Annu. Rev. Nucl. Part. Sci. **60**, 1 (2010).
[18] M. Burkardt, Phys. Rev. D **62**, 071503 (2000); **66**, 119903 (E) (2002); Int. J. Mod. Phys. A **18**, 173 (2003).
[19] M. Diehl, Eur. Phys. J. C **25**, 223 (2002); **31**, 277(E) (2003).
[20] L. Frankfurt, G. A. Miller, and M. Strikman, Nucl. Phys. **A555**, 752 (1993); Annu. Rev. Nucl. Part. Sci. **44**, 501 (1994).
[21] G. P. Lepage and S. J. Brodsky, Phys. Rev. D **22**, 2157 (1980).
[22] I. V. Musatov and A. V. Radyushkin, Phys. Rev. D **56**, 2713 (1997).
[23] S. Kumano, M. Strikman, and K. Sudoh, Phys. Rev. D **80**, 074003 (2009); S. Kumano and M. Strikman, Phys. Lett. B **683**, 259 (2010).
[24] G. Bertsch, S. J. Brodsky, A. S. Goldhaber, and J. F. Gunion, Phys. Rev. Lett. **47**, 297 (1981).
[25] L. Frankfurt, G. A. Miller, and M. Strikman, Phys. Lett. B **304**, 1 (1993).
[26] L. Frankfurt, G. A. Miller, and M. Strikman, Found. Phys. **30**, 533 (2000); Phys. Rev. D **65**, 094015 (2002).
[27] E. M. Aitala *et al.* (E791 Collaboration), Phys. Rev. Lett. **86**, 4773 (2001).
[28] B. Clasie *et al.*, Phys. Rev. Lett. **99**, 242502 (2007).
[29] G. A. Miller and M. Strikman, Phys. Rev. C **82**, 025205 (2010).
[30] S. Venkat, J. Arrington, G. A. Miller, and X. Zhan, arXiv:1010.3629.
[31] J. D. Bjorken and S. D. Drell, *Relativistic Quantum Fields* (McGraw-Hill, New York, 1965).
[32] Use of a subtracted dispersion relation in Eq. (1) would lead to an expression for the transverse density that differs from Eq. (3) by a delta function $\delta^{(2)}(\boldsymbol{b})$. Subtractions therefore have no influence on the dispersion result for the transverse density at finite b.
[33] M. Strikman and C. Weiss, Phys. Rev. C **82**, 042201 (2010).
[34] C. Bruch, A. Khodjamirian, and J. H. Kuhn, Eur. Phys. J. C **39**, 41 (2005).
[35] G. J. Gounaris and J. J. Sakurai, Phys. Rev. Lett. **21**, 244 (1968).
[36] Reference [34] also provides an alternative fit in which the resonances are described by the BW form. As mentioned above, the BW form has a spurious branch cut singularity at $t = 0$, which in the full GS form is canceled by the off-shell term. This has the consequence that the imaginary part obtained with the BW parameters of Ref. [34] does not satisfy the normalization condition $\pi^{-1}\int_{4m_\pi^2}^{\infty} dt' \,\mathrm{Im}F_\pi(t')/t' = 1$ exactly, but with a small discrepancy related to the spectral strength on the unphysical cut (the BW ansatz in [34] was normalized to unit value at $t = 0$, not to unit integral over the imaginary part). In our dispersion analysis we therefore use the GS parametrization, which has the correct analyticity structure and is free of this problem.
[37] C. A. Dominguez, Phys. Lett. B **512**, 331 (2001).
[38] This argument assumes that the change of $\mathrm{Im}F_\pi(t)$ does not substantially alter the cancellation of successive resonance contributions implied by the dual resonance picture. The effect of an "unbalanced" resonance will be estimated separately below.
[39] We note that the fit of Ref. [34] also does not reproduce the value of $|F_\pi|^2$ at $\sqrt{t} = 3.1$ GeV extracted from the $J/\psi \to \pi\pi$ decay; see Ref. [34] for a critical discussion of this datum.
[40] J. S. Conway *et al.*, Phys. Rev. D **39**, 92 (1989).
[41] The valence quark density in Eq. (10) is assumed to be normalized to unit integral, $\int dx q_\pi(x) = 1$. Note, however, that Eq. (10) is intended as a model for large-x configurations and should be integrated only over this region.
[42] M. Gluck, E. Reya, and I. Schienbein, Eur. Phys. J. C **10**, 313 (1999).
[43] M. A. B. Beg and A. Zepeda, Phys. Rev. D **6**, 2912 (1972).
[44] J. Gasser and H. Leutwyler, Ann. Phys. (N.Y.) **158**, 142 (1984).
[45] J. Gasser and U. G. Meissner, Nucl. Phys. **B357**, 90 (1991).
[46] D. Diakonov and V. Y. Petrov, Nucl. Phys. **B272**, 457 (1986).
[47] P. Faccioli, A. Schwenk, and E. V. Shuryak, Phys. Rev. D **67**, 113009 (2003).
[48] L. Frankfurt, M. Strikman, and M. Zhalov, Acta Phys. Pol. B **34**, 3215 (2003).